24th IMEKO TC4 International Symposium
22nd International Workshop on ADC and DAC Modelling and Testing
IMEKO TC-4 2020
Palermo, Italy, September 14-16, 2020

Effect of noise and partial synchronization on amplitude measurement of multiple Chirp Spread Spectrum signals

Antonio Moschitta, Antonella Comuniello, Alessio De Angelis, F. Santoni, Paolo Carbone

University of Perugia, Department of Engineering, Via G. Duranti 93, 06125 Perugia (PG), Italy
{antonio.moschitta,alessio.deangelis,francesco.santoni,paolo.carbone}@unipg.it,
antonella.comuniello@studenti.unipg.it

***Abstract* – In this paper, simultaneous amplitude measurement of multiple Chirp Spread Spectrum (CSS) signals is discussed. CSS signals are assumed to be generated by digital devices whose clocks are not fully synchronized. The effects of incomplete synchronization and noise at the receiver side are investigated and discussed, assuming that the signals' amplitudes are estimated using correlation techniques.**

I. INTRODUCTION

Simultaneous transmission and detection of multiple waveforms is an enabler for various practical applications, ranging from telecommunication to Internet of Things and smart sensors. An example is the deployment of sensor networks, that support several monitoring and location-based applications [1-3]. Provided that an accurate propagation model is known, and that a known waveform is transmitted from a set of known positions, parametric characterization of the received waveforms permits both area monitoring and positioning. In this regards, simultaneous measurement of multiple waveforms is a desirable feature, supporting for instance real-time tracking of multiple objects. To this aim, Multiple Access schemes based on time, frequency, or code orthogonality were proposed, leading to many Time Division Multiple Access (TDMA), Frequency Division Multiple Access (FDMA), and Code Division Multiple Access solutions (CDMA) [4]. A typical problem when the multiple waveforms coexist in the time domain is the Multiple Access Interference (MAI), introduced because the set of waveforms used in practical applications are not fully orthogonal to each other [5-6]. This problem may be mitigated, using for instance Successive Interference Cancellation (SIC) algorithms [5-6].

However, while the available literature is focused on reliable extraction of digital information carried by the transmitted waveforms, less attention was given to accurate parametric characterization of multiple waveforms, simultaneously received in a noisy environment.

In this paper, the latter problem is analyzed, assuming that the transmitted waveforms are a set of Chirp Spread Spectrum (CSS) signals [7-8]. CSS signals were recently introduced and adopted in commercial solutions like LoRa, since they provide good correlation properties (i.e. narrow auto-correlation pulses and a very low cross-correlation) and robustness to noise [9-18]. They are claimed to support wireless sensor networks covering areas up to a few km.

Measurement of the amplitude of multiple received CSS signals is discussed, assuming that the receiver estimates the amplitude of the desired waveform using correlation techniques [5][19-20]. The analysis is carried out under the hypothesis that the transmitting devices are not fully synchronized, that is by assuming that the transmitted CSS waveforms are generated using direct digital synthesis and that the clocks of the transmitters are not in phase. The analysis was carried out assuming a noisy environment and two different correlation techniques, the second one attempting to refine the first using quadratic interpolation [15].

II. CSS SIGNAL MODEL AND AMPLITUDE ESTIMATION

A. Signal model

The considered CSS waveforms are a set of N linear chirp pulses, obtained from a base signal $s_0(\cdot)$ with unitary amplitude that spans the frequency interval $[f_L,f_H[$ in a time T, such that

$$s_0(t) = \begin{cases} \sin\left(2\pi\left(f_L + \frac{1}{2}\frac{f_H - f_L}{T}t\right)t\right), & 0 \le t < T \\ 0, & elsewhere \end{cases} \quad (1)$$

A set of N CSS pulses can be obtained by applying circular shifts of multiples of $\tau=T/N$ to $s_0(\cdot)$, such that the n-th CSS signal $s_n(\cdot)$ is given by

$$s_n(t) = s_0\left(\left\langle\frac{t-\tau_n}{T}\right\rangle T\right), \; n = 0,..,N-1, \quad (2)$$

$$\tau_n = n\tau, \quad n = 0,\dots,N-1, \quad (3)$$

where $\langle\cdot\rangle$ is the fractional part operator, defined as $\langle x\rangle = x - \lfloor x\rfloor$, and $\lfloor\cdot\rfloor$ is the floor operator [21]. The

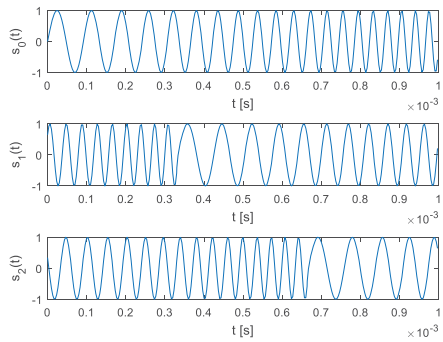

Fig. 1– A set of 3 *CSS signals, spanning the frequency interval* [10 kHz, 30 kHz] *in* 1ms.

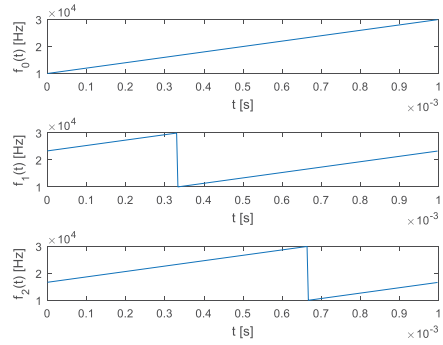

Fig. 2 – Instantaneous frequencies corresponding to the signals in Fig. 1.

instantaneous frequency of the *n*-th CSS pulse is given by

$$f_n(t) = f_0\left(\left\langle\frac{t-\tau_n}{T}\right\rangle T\right), \qquad 0 \le t < T. \quad (4)$$

where $f_0(t) = f_L + \frac{(f_H - f_L)t}{T}$, $0 \le t < T$ describes the instantaneous frequency of the base signal $s_0(\cdot)$.

As an example, a set of N=3 CSS signals and the corresponding instantaneous frequencies, obtained for f_L=10 kHz, f_H=30 kHz, and T=1ms are shown in Figs. 1 and 2.

The considered received signal $s_R(\cdot)$ is the superimposition of N CSS pulses with different amplitudes, not fully synchronized, and affected by an Additive White Gaussian Noise (AWGN) $n(\cdot)$ with standard deviation σ, and can be modeled as

$$s_R(t) = \sum_{n=0}^{N-1} s_{Rn}(t - d_n) + n(t), \quad (5)$$

$$s_{Rn}(t) = A_n s_n(t), \quad n=0,\ldots,N\text{-}1. \quad (6)$$

where A_n is the amplitude of the n-th CSS pulse at the receiver input, while d_n models the lack of synchronization as a random delay. In the following, d_n was assumed uniformly distributed in $[0,d_{max}]$.

B. Measurement model and procedure

The receiver samples $s_R(\cdot)$ at a frequency f_S, obtaining a sequence $s_R[k]$, k=0,…,M-1. In order to estimate A_n, a sampled replica of the normalized signal $s_n(\cdot)$ is stored in the receiver, defined as

$$s_n[k] = s_n(kT_S),\ T_S = 1/f_S,\ \ k = 0,..,M-1. \quad (7)$$

Then, the receiver computes the cross-correlation sequence $C_{Rn,n}[\cdot] = s_{Rn} \star s_n$ between the received signal $s_{Rn}[k]$ and $s_n[k]$, where $\star$ denotes the cross-correlation operator, and finds $C_{n,max}$, defined as

$$C_{n,max} = max\left(C_{Rn,n}[k]\right), k = 0, \ldots, 2M-1. \quad (8)$$

that is the maximum observed value in the correlation sequence. If a single CSS pulse were transmitted and if $s_{Rn}[\cdot]$ and $s_{Rn}[\cdot]$ were synchronized, $C_{n,max}$ would be obtained as

$$C_{n,max} = \sum_{k=0}^{M-1} s_{Rn}[k]s_n[k] = A_n \sum_{k=0}^{M-1} s_n[k]^2, \quad (9)$$

where A_{Rn} is the amplitude of the n-th received CSS pulse. Finally, by approximating the power of a linear chirp pulse with peak amplitude A as $A^2/2$, A_n can be estimated as

$$\hat{A}_n = \frac{2}{M} C_{n,max}, \quad (10)$$

Note that the peak estimation accuracy may be improved by applying interpolation techniques to the maximum $C_{n,max}$, and to its neighboring samples.

When multiple CSS signals are superimposed, multiple peaks will appear in the cross-correlation sequence, because, for $m \neq n$, a pulse $s_n(\cdot)$ can be obtained by applying a circular shift $(n\text{-}m)\,\tau$ to the pulse $s_m(\cdot)$. However, if the transmissions of synchronized, the position of the correct peak is known in advance, falling in the middle of the cross-correlation sequence. For instance, if $C_{Rn,n}[\cdot]$ is stored as vector accessed with an index ranging from 0 to 2M-2, and M is even, the correct correlation peak occurs in k=M-1. Note that correlation peaks due to CSS signals belonging to the set defined by (1) and (2) are spaced from each other by integer multiples of τ/T_S. This knowledge can be used by the receiver to restrict the maximum search in the sequence $C_{Rn,n}[\cdot]$ to a neighborhood of the expected peak position.

It is also worth noting that the CSS signals feature good correlation properties but are not fully orthogonal to each other. Consequently, the residual cross-correlation between different CSS signals acts as an uncertainty source on the amplitude estimation, especially when the signals' amplitudes are much different from each other.

III. SIMULATION RESULTS

The effectiveness of the proposed amplitude measurement was investigated under various conditions. A set of N=10 CSS signals was considered, with f_L=38 kHz, f_H =42 kHz, and T=0.1s, leading to the received signal (5). The selected CSS parameters are compatible with the characteristics of ultrasound transducers, used in previous research activities, focused on positioning

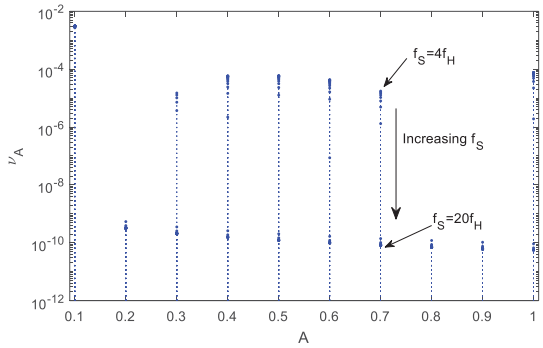

Fig. 3 – Amplitude estimation error, as a function of sampling frequency and chirp amplitude, in absence of noise and synchronization error, when correlation peaks are estimated using a simple maximum search on the correlation envelope. For each amplitude A, the largest value ν_A in the stem plot is obtained for $f_S=4f_H$, and monotonically decreases when f_S is increased.

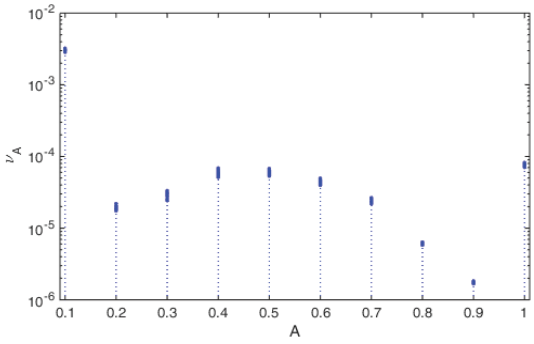

Fig. 4 – Amplitude estimation error, as a function of sampling frequency and chirp amplitude, in absence of noise and synchronization error, when quadratic interpolation is used to estimate the correlation peaks.

systems [15]. The analysis was carried out using Monte Carlo simulations, modeling four basic scenarios, assuming transmission in absence of AWGN and synchronization error, in presence of AWGN alone, in presence of synchronization error alone, and in presence of both AWGN and synchronization error. In all these cases two methods for estimating the correlation peaks were considered. The first one was based on a simple maximum search, the second one based on a 3-point quadratic interpolation algorithm, fed by the maximum observed value in the correlation sequence and its adjacent samples. The analysis, based on Monte Carlo simulations of 1000 iterations, was repeated for 25 different values of the sampling frequency f_S, linearly spaced in the interval $[4f_H, 20f_H]$. The dependence on sampling frequency was investigated, as a mean of assessing a minimum requirement on such parameter.

Use of quadratic interpolation was explored as a possible mean to relax the requirement on the sampling frequency, without significantly increasing the computational complexity of the receiver algorithms. Finally, the analysis was carried out by assuming N=10 CSS signals with linearly spaced amplitudes, that is A_n=0.1(n+1), n=0,…,9. The selected case is more significant in practical scenarios, where a set of signals with very different amplitudes may be received.

To compare the results emerging from the different scenarios, the rms of the normalized amplitude estimation error ν_{rms} was evaluated and used as a meaningful performance metric. In particular, ν_{rms} is defined as

$$\nu_{rms} = \frac{1}{A}\sqrt{m_{e_A}^2 + \sigma_{e_A}^2}, \quad (11)$$

where, for each given CSS signal amplitude A and sampling frequency f_S, m_{e_A} and $\sigma_{e_A}^2$ are respectively the sample mean and the sample variance of the amplitude estimation error e_A, evaluated across the population of 1000 Monte Carlo simulation results. Note that can be also seen as the rms value of the relative amplitude error defined as

$$\nu_A = \frac{\hat{A}-A}{A}, \quad (12)$$

where $\hat{A}$ is the estimator of the amplitude A.

A. No AWGN, no synchronization error

This analysis, run in absence of random contributions, is not a Monte Carlo analysis, but shows the asymptotic performance when perfect synchronization between the CSS signals is achieved in a noiseless scenario.

The analysis was initially run assuming transmission of a single CSS pulse. In this case, each amplitude was estimated with a relative error ν_A ranging between 10^{-10} and 10^{-16}. Conversely, when simultaneous measurement of the 10 CSS signals was considered, the results in Fig. 3 and 4 were obtained, where the stem plots show the relative estimation error ν_A as a function of each chirp amplitude A_n, n=0,…,N-1. For each of the 10 CSS amplitudes, 25 points are shown, obtained by increasing the sampling frequency from $f_S=4f_H$=168 ksample/s to $f_S=20f_H$=840 ksample/s. Fig. 3 was obtained by assuming that, prior using (10) to estimate A_n, each correlation peak $C_{n,max}$ was estimated using a maximum search on the envelope $C_{Rn,n}[\cdot]$. Note that ν_A monotonically decreases when f_S is increased from $4f_H$, to $20f_H$. Conversely, Fig. 4 was obtained using a quadratic interpolation to refine the estimation of $C_{n,max}$ before using (10). All the chirp signals were estimated with $\nu_A=10^{-5}$ or better, except for the lowest amplitude A_0=0.1 that was estimated with $\nu_A = 3\cdot10^{-3}$. Using interpolation did not improve the estimation accuracy. The increase in the relative estimation error is due to MAI. Using quadratic interpolation when estimating the correlation peak $C_{n,max}$ to be used in (10) did not improve the estimation accuracy with respect to the simple max search (9). Moreover, the estimation accuracy does not improve when the sampling frequency is increased.

B. No AWGN, synchronization error

This set of simulations aimed at assessing the effect of incomplete synchronization alone between the N=10 transmitters and the receiver. As anticipated in section II, the lack of synchronization was modeled by the random delay d_n in (5), assumed to be a realization of a random

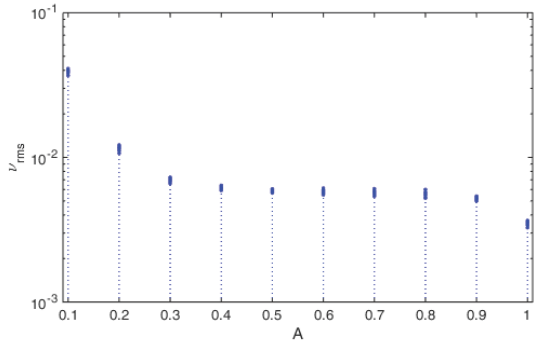

Fig. 5 - Amplitude estimation error, as a function of sampling frequency and chirp amplitude, in absence of noise and for d_{max}=8·10^{-3}T.

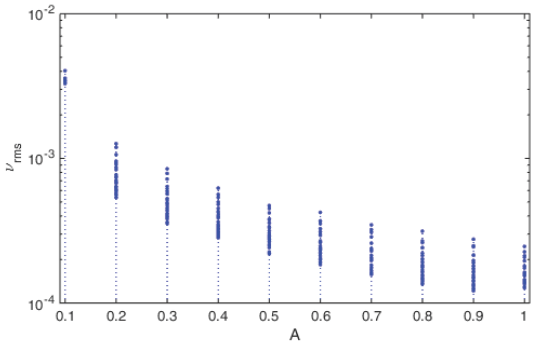

Fig. 6 - Amplitude estimation error, as a function of sampling frequency and chirp amplitude, in presence of noise (σ=2.24·10^{-2}) and in absence of synchronization errors (d_{max}=0).

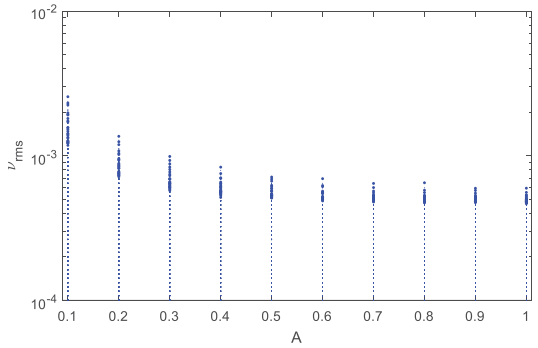

Fig. 7 - Amplitude estimation error, when a single CSS pulse is transmitted, as a function of chirp amplitude, in presence of both noise (σ=2.24·10^{-2}) and synchronization errors (d_{max}=8·10^{-3}T).

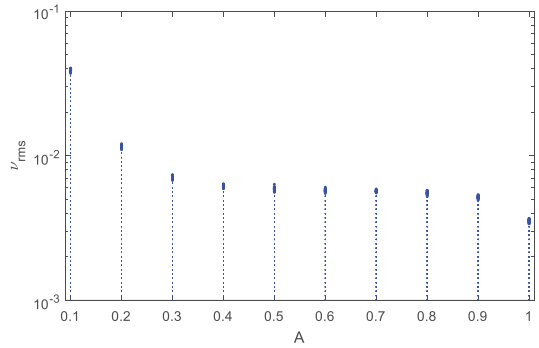

Fig. 8 - Amplitude estimation error, when 10 CSS pulses are simultaneously transmitted, as a function of chirp amplitude, in presence of both noise (σ=2.24·10^{-2}) and synchronization errors (d_{max}=8·10^{-3}T).

variable, uniformly distributed in [-d_{max},d_{max}] with d_{max}=8·10^{-3}T=8·10$^{-2}\tau$. While d_{max} is just 8% of the minimum spacing τ between different peaks in the correlation sequence $C_{Rn,n}[\cdot]$, it may amount, depending on the sampling frequency, up to a few tens of samples. Note that the interpolation technique did not improve the maximum search estimator, leading to identical accuracy.

The analysis results are shown in Fig. 5. By comparing Fig. 5 with Figs. 3 and 4 it can be observed that the considered synchronization errors reduce the accuracy by one order of magnitude, and that the sensitivity to MAI is increased. In fact, now also the CSS signal with A_2=0.2 is estimated with a significantly reduced accuracy with respect to larger signals, and the estimation accuracy slightly increases for the CSS signals featuring a larger amplitude. As for the previous case, increasing the sampling frequency and using quadratic interpolation in the correlation analysis did not significantly affect the estimation accuracy.

C. AWGN, no synchronization error

In this scenario, complementary to the previous one, AWGN was assumed at the receiver input, in presence of perfect synchronization (d_{max}=0) between the N transmitters and the receiver. The noise level was set by σ=2.24·10^{-2}, corresponding to a Signal to Noise Ratio (SNR) of 10 dB for the weakest CSS signal with A_0=0.1, growing to 20 dB for the strongest CSS signal with A_9=1. The results are shown in Fig. 6. With respect to the ideal case summarized by Figs. 3 and 4, a small accuracy reduction can be observed, since the relative estimation error is still in the order of 10^{-3}. Conversely, a comparison with Fig. 5 show that the estimator accuracy improves more when the sampling frequency f_S is increased. This suggests that the estimator is more sensitive to synchronization errors than to noise.

D. AWGN and synchronization errors

This set of simulation was focused on assessing the joint effect of noise and synchronization errors, aiming at modeling a practical scenario. While keeping a constant noise level (σ=2.24·10^{-2}) various levels of synchronization error were tested, with d_{max} ranging from 10^{-4}T to 8·10^{-3}T. Transmission of a single CSS signal and of multiple CSS signals were tested. When testing the estimation of a single CSS, the observed accuracy ν_{rms}

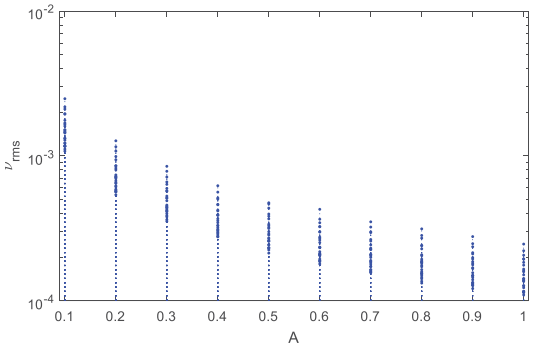

Fig. 9 - Amplitude estimation error, when a single CSS pulse is transmitted, as a function of chirp amplitude, in presence of both noise (σ=2.24·10^{-2}) and synchronization errors (d_{max}=10^{-4}T).

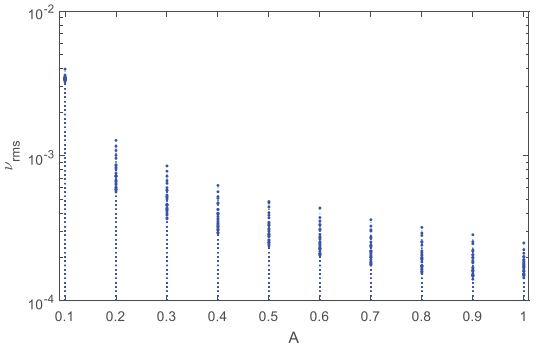

Fig. 10 - Amplitude estimation error, when 10 CSS pulses are simultaneously transmitted, as a function of chirp amplitude, in presence of both noise (σ=2.24·10^{-2}) and synchronization errors (d_{max}=10^{-4}T).

was in the order of 10^{-3} and increasing the sampling frequency perceivably improved the estimation accuracy of weak signals, as shown in Fig. 7.

However, when multiple CSS pulses are transmitted, Fig. 8 shows that accuracy is further reduced by MAI by an order of magnitude. Moreover, by comparing results for different values of d_{max} it was also observed that the accuracy gain obtained by increasing the sampling frequency is progressively reduced when the synchronization error increases. For instance, Fig. 8 shows that for d_{max}=8·10^{-3}T increasing the sampling frequency does not strongly affect the estimation accuracy. Simulation results also show that when synchronization error is negligible, the ν_{rms} obtained when multiple CSS pulse are simultaneously transmitted approximates that obtained when a single CSS pulse is transmitted. This can be observed by comparing Figs. 9 and 10, obtained for σ=2.24·10^{-2} and d_{max}=10^{-4}T, to Figs. 7 and 8, obtained for σ=2.24·10^{-2} and d_{max}=8·10^{-3}T. Note that d_{max}=10^{-4}T corresponds to a synchronization error within the sampling period T_S. Once again, using quadratic interpolation did not improve the accuracy with respect to applying a simple max search to the correlation sequence $C_{Rn,n}[\cdot]$.

IV. DISCUSSION

The compared analysis shows that both noise and synchronization errors increase the sensitivity to MAI, perceivably reducing the estimation accuracy for low level CSS signals. It can also be inferred that noise effects on estimation accuracy may be partially mitigated by increasing the sampling frequency. Conversely, when synchronization errors are introduced the estimation accuracy achieved in presence of simultaneous transmission of multiple CSS signals is less sensitive to sampling frequency. When both noise and synchronization errors are introduced, the latter dominates the sensitivity of the estimation accuracy to variations in the sampling frequency. This is an

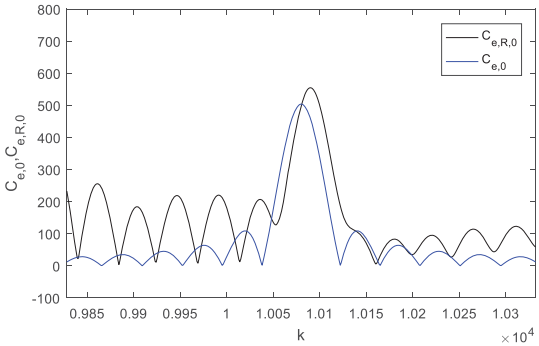

Fig. 11 – Effect of synchronization error, under the conditions of Fig. 10. The peak index of the cross correlation envelope $C_{e,r,0}$ generated by the received signal and s_0 $s_0(\cdot)$ is shifted with respect to that obtained from the autocorrelation envelope $C_{e,0}$ of $s_0(\cdot)$

interesting result, since in IoT based applications CSS signals may be generated and collected by low power microcontrollers, such that high sampling frequency may not be easily achieved. These results also suggest that the measurement may be optimized by reducing the synchronization error to the sampling period T_S or less.

Finally, the considered 3-point quadratic interpolation did not appear to perceivably improve the estimation accuracy when noise or inaccurate synchronization between the transmitting nodes are present, leading in some cases to an accuracy loss. This behavior may be explained by observing that in presence of synchronization errors, as shown by Fig. 11, the peak of the correlation between the received signal and the selected decoding signal do no longer occur in the expected position. In addition MAI may introduce additional errors, due to the tails of cross correlations between the desired signal and other CSS interferers. This would in turn reduce the accuracy of any interpolation technique based on samples in a neighborhood of the peak value, especially for low amplitude signals disturbed by stronger interferers.

V. CONCLUSIONS

Amplitude parametric characterization of multiple CSS signals with different amplitudes was investigated, analyzing the achievable accuracy as a function of noise and synchronization errors between the multiple transmitters and the receiver. A compared analysis was run, assessing the individual and joint effect of noise and synchronization errors. It was shown that, in presence of MAI and synchronization errors, interpolation techniques may be ineffective as a mean to improve the peak estimation in correlation sequences. It was also shown that increasing sampling frequency may not lead to a significant accuracy improvement in presence of significant synchronization errors.

VI. ACKNOWLEDGEMENTS

This research activity was partially funded through grant *Identificazione e caratterizzazione accurata di sistemi e segnali*, Ricerca di Base 2018 and 2019- University of Perugia, Department of Engineering.

REFERENCES

[1] S. Park, B. Shim and J. W. Choi, "Iterative Channel Estimation Using Virtual Pilot Signals for MIMO-OFDM Systems," *IEEE Trans. on Signal Processing*, vol. 63, no. 12, pp. 3032-3045, June15, 2015.

[2] L. Svilainis, A. Rodriguez-Martinez, A. Chaziachmetovas and A. Aleksandrovas, "Application of binary excitation spread spectrum signals for spectral compensation," IEEE IDAACS 2017, Bucharest, pp. 1105-1110.

[3] J. Wang, Q. Gao, Y. Yu, H. Wang and M. Jin, "Toward Robust Indoor Localization Based on Bayesian Filter Using Chirp-Spread-Spectrum Ranging," *IEEE Trans. on Industrial Electronics*, vol. 59, no. 3, pp. 1622-1629, March 2012.

[4] G. De Angelis, A. De Angelis, A. Comuniello, A. Moschitta and P. Carbone, "Simultaneous RSS Measurements Using Multiple Inductively Coupled Coils," IEEE M&N 2019, Catania, Italy, 2019, pp. 1-6.

[5] A. Moschitta, A. Comuniello, F. Santoni, A. De Angelis, P. Carbone, M.L. Fravolini, "Simultaneous amplitude measurement of multiple Chirp Spread Spectrum signals," IEEE I2MTC 2020, Dubrovnik, Croatia, May 25-28, 2020.

[6] M. A. B. Temim, G. Ferré, B. Laporte-Fauret, D. Dallet, B. Minger and L. Fuché, "An Enhanced Receiver to Decode Superposed LoRa-like Signals," IEEE *Internet of Things Journal*, pp. 1-1, 08 April 2020, DOI: 10.1109/JIOT.2020.2986164.

[7] A. De Angelis et al., "On the Use of Magnetically Coupled Resonators for Chirp-Based Timestamping," *IEEE Trans. on Instrumentation and Measurement*, vol. 64, no. 12, pp. 3536-3544, Dec. 2015.

[8] A. De Angelis, P. Carbone, E. Sisinni and A. Flammini, "Performance Assessment of Chirp-Based Time Dissemination and Data Communications in Inductively Coupled Links," *IEEE Trans. on Instrumentation and Measurement*, vol. 66, no. 9, pp. 2474-2482, Sept. 2017.

[9] https://lora-alliance.org/, retrieved on the internet as of 26/11/2019.

[10] H. Hur and H. Ahn, "A Circuit Design for Ranging Measurement Using Chirp Spread Spectrum Waveform," *IEEE Sensors Journal*, vol. 10, no. 11, pp. 1774-1778, Nov. 2010.

[11] Sze Fong Yau and Y. Bresler, "Worst-case Cramer-Rao bound for parametric estimation of superimposed signals," Fifth ASSP Workshop on Spectrum Estimation and Modeling, Rochester, NY, USA, 1990, pp. 187-191.

[12] S. Changyin and B. Zhang, "Super-resolution algorithm for instantaneous ISAR imaging," *Electronics Letters*, vol. 36, no. 3, pp. 253-255, 3 Feb. 2000.

[13] B. Friedlander and J. M. Francos, "Estimation of amplitude and phase parameters of multicomponent signals," *IEEE Trans. on Signal Processing*, vol. 43, no. 4, pp. 917-926, April 1995.

[14] A. Rao and R. Kumaresan, "Separation of cochannel signals using the parametric constant modulus algorithm," 1996 IEEE International Conference on Acoustics, Speech, and Signal Processing Conference Proceedings, Atlanta, GA, USA, 1996, pp. 2686-2689 vol. 5.

[15] A. De Angelis, A. Moschitta, P. Carbone, M. Calderini, S. Neri, R. Borgna, M. Peppucci, "Design and Characterization of a Portable Ultrasonic Indoor 3-D Positioning System," *IEEE Trans. on Instrumentation and Measurement*, Vol. 64, No. 10, pp. 2616 – 2625, Oct. 2015. DOI: 10.1109/TIM.2015.2427892.

[16] G. Cerro et al., "An Accurate Localization System for Nondestructive Testing based on Magnetic Measurements in quasi-planar domain," *Measurement*, vol. 139, pp. 467-474, June 2019.

[17] R. Demirli and J. Saniie, "A generic parametric model for ultrasonic signal analysis," 2009 IEEE International Ultrasonics Symposium, Rome, 2009, pp. 1522-1525.

[18] C. M. De Dominicis, P. Pivato, P. Ferrari, D. Macii, E. Sisinni and A. Flammini, "Timestamping of IEEE 802.15.4a CSS Signals for Wireless Ranging and Time Synchronization," *IEEE Trans. on Instrumentation and Measurement*, vol. 62, no. 8, pp. 2286-2296, Aug. 2013.

[19] Y. Zhou, P. He, S. Ji and L. Zhu, "Quasi-Orthogonal Chirp Signals Design for Multi-User CSS System," 2009 First International Conference on Information Science and Engineering, Nanjing, 2009, pp. 631-634.

[20] M. K. Varanasi and B. Aazhang, "Multistage detection in asynchronous code-division multiple-access communications," *IEEE Trans. on Communications*, vol. 38, no. 4, pp. 509-519, April 1990.

[21] Graham, Ronald L.; Knuth, Donald E.; Patashnik, Oren (1992), Concrete mathematics: a foundation for computer science, Addison Wesley, p. 70, ISBN 0-201-14236-8.